

Hydroxyapatite/Fe₃O₄ Nanocomposite as Efficient Sorbent for the Extraction of Phthalate Esters from Water Samples

M. Chahkandi* and A. Amiri

Department of Chemistry, Faculty of Sciences, Hakim Sabzevari University, 9617976487 Sabzevar, Iran

(Received 8 May 2019, Accepted 6 July 2019)

In this study, we demonstrate the application of newly developed magnetic potassium substituted hydroxyapatite (KHA/Fe₃O₄) for the extraction of phthalate esters (PE) from water samples. Nanoparticles of KHA were synthesized through an easy alkoxide-based sol-gel technique. The structure of nanocomposite was characterized by X-ray diffraction (XRD), Fourier transform infrared (FTIR) analysis, and energy dispersive X-ray Analysis (EDXA). Moreover, the size of nanoparticle and micro-strain of synthesized KHA and KHA/Fe₃O₄ using Williamson-Hall (W-H) plots and transmission electron microscopy (TEM) were measured. The hexagonal and cubic structures of synthesized KHA and its nanocomposite having P6₃/m space group confirmed by XRD pattern. Also, the size of spherical particles of KHA in pure and nanocomposite, and Fe₃O₄ nanoparticles evaluated by W-H and TEM methods are in good agreement as 60, 65 and 18 nm. The PEs were analyzed by gas chromatography-flame ionization detector (GC-FID). Different parameters influencing the extraction efficiency including: sample pH, amount of sorbent, extraction time, desorption conditions, and salt effect, were optimized. The obtained optimal conditions were: sample pH, 7; amount of sorbent, 25 mg; extraction time, 8.0 min; desorption solvent and its volume, 200 μ l dichloromethane; and desorption time, 5.0 min. Under optimum conditions, good linearity was achieved for all analytes in the 0.015-100 ng ml⁻¹ concentration range. The limits of detection (at an S/N ratio of 3) are between 0.005 and 0.03 ng ml⁻¹. The recoveries of PEs from spiked real water samples are between 86.3 and 99.2%, with relative standard deviations between 5.3 and 9.3%.

Keywords: Phthalate esters, Gas chromatography, Potassium substituted hydroxyapatite, Magnetic nanoparticle, Sol-gel, Transmission electron microscopy, Fourier transform infrared spectrometry, X-ray diffraction

INTRODUCTION

Phthalate esters (PEs) are well-known plastic materials' additives to increase their flexibility and workability through weak secondary molecular interactions with polymer chains. PEs are usually just non-covalently bond plasticizers that's why they are easy to leach [1,2]. In recent years, many research articles have appeared that discuss the impact of PEs on wild animals and humans [3-6]. Some studies have reported that PEs exhibit acute or chronic toxicity toward aquatic organisms [7]. Furthermore, some PEs are classified as suspected carcinogens [8]. The extensive use has created a widespread alarm for both the

human health and the environment.

So far, the development of the analytical procedures to determine the presence of PEs in environmental samples has received much attention in recent years. The most widely used methods for the determination of PEs have been chromatographic techniques, such as gas chromatography (GC) [9] and high-performance liquid chromatography (HPLC) [10,11]. The reported sample preparation methods for the extraction of PEs include solid-phase microextraction (SPME) [12], hollow-fiber liquid-phase microextraction (HF-LPME) [13], stir-bar sorptive extraction (SBSE) [14], and dispersive liquid-liquid microextraction (DLLME) [15]. Recently, new SPE technique based on the use of magnetic nanoparticles, called magnetic solid phase extraction (MSPE) has been

*Corresponding author. E-mail: m.chahkandi@hsu.ac.ir

introduced for separation and preconcentration of organic and inorganic species from complex matrixes. An appropriate MSPE adsorbent is very crucial for the efficient extraction of the analytes, therefore the exploration of new adsorbents has received growing attention [16,17].

Hydroxyapatite (HA) bioceramic as the useful Calcium Phosphate (Ca-P) compound has attracted high attention because of low-cost preparation, non-toxicity, and high adsorptive capabilities, possess various, interesting, and applicable bio-properties including: hard tissue repairing [18], drug delivery [19], dentistry [20], antitumor [21], cell proliferation [22], protein adsorption [23], capturing of heavy metal and organic pollutants [24,25], and photocatalysis [26]. HA and its derivatives including two ionic C and P binding sites on the surfaces of unite cell that rich in cationic and phosphate ions, respectively [27] well known as the good absorbent for many anionic and cationic compounds [28,29]. However, researchers try to optimize and enhance these amazing abilities by making new nanocomposites and/or elemental substituted of HA. The doping or cation substitution in HA can occur instead of calcium ions, phosphate groups or hydroxyl groups [30]. Copper substituted HA about the uranium [31,32], Ag-doped HA about the Congo red [33], HA loaded with strontium about the soybean oil [34], and silicon doped HA for copper [35] adsorption, and so on can be mentioned. Potassium has capability in the regulation of biochemical and apatite mineral nucleation processes [36,37]. K-substituted HA should be a better material comparing the individual HA or β -tri calcium phosphate about the biomineralization process [38]. Introducing new composites of HA including inorganic or organic hybrids has opened up a new arena like bio-microreactor for synthesis of biocompatible materials [39], bone tissue engineering [40-42], healing of bone fractures [43], magnetic [44], high defluoridation capacity [45], drug delivery [46], and so on.

Beside different preparation methods of HA, sol-gel technique due to simplicity, facility to make nano-compounds, purity of products, the low temperature of thermal treatment, and low crystallinity of the product has attracted much attention [47-49]. However, there are no reports, about synthesise of sol-gel-derived K-substituted HA (KHA). Herein, the new synthesized sol-gel-derived KHA and its magnetic nanocomposite KHA/Fe₃O₄

introduced as an effective sorbent for the extraction and preconcentration of phthalate esters from aqueous samples. The prepared nanomaterials were studied by powder X-ray diffraction (XRD), energy dispersive X-ray analysis (EDXA), Fourier transform infrared (FTIR) spectroscopy, and particle size estimated by XRD and transmission electron microscopy (TEM).

EXPERIMENTAL

Chemicals and Materials

Phthalate ester compounds include dimethyl phthalate (DMP), diethyl phthalate (DEP), di-isobutyl phthalate (DIBP), di-n-butyl phthalate (DnBP), and di-2-ethylhexyl phthalate (DEHP) were purchased from Sigma-Aldrich Chemical Company. All reagents and solvents were obtained from Merck and Sigma-Aldrich chemical companies and used without purification. The stock solutions of containing PEs each at 100 mg l⁻¹ were prepared in methanol and stored in a refrigerator at 4 °C.

Instrumentation

The analyses of the PEs were carried out on Shimadzu-17A GC system (Tokyo, Japan) equipped with a capillary split/splitless injector system and flame ionization detection (FID) system, on a Hicap CBP-5-M25-025 (5% biphenyl + 95% polydimethylsiloxane) fused-silica column (25 m, length; 0.25 mm I.D.; 0.22 μ m, film thickness). The temperatures of injector and detector were maintained at 300 and 300 °C, respectively. Nitrogen (99.999%) was used as the carrier gas with a constant flow of 1 ml min⁻¹. The oven temperature was held at 100 °C for 2 min, increased to 200 °C at a rate of 15 °C min⁻¹, then raised to 280 °C at a rate of 10 °C min⁻¹ and held for 4 min. Phase identification and characterization of the calcined gel of KHA and KHA/Fe₃O₄ nanocomposite were performed using the X-ray diffractometer (XRD, Philips, X'pert Pro, Cu K α) at a scanning speed of 1° 2 θ /min from 20 to 45° and IR spectroscopy (Buck 500, KBr) in the range of 500-4000 cm⁻¹. Particle size distribution was determined by TEM observations. TEM (Leo 912 AB-Germany) equipped with a thermionic gun and was operated at 120 kV. TEM sample was prepared as follows: the powder of samples was ultrasonically dispersed for 2 h in absolute

ethanol and afterward deposited on a carbonated copper grid. Moreover, particle size and micro-strain of KHA and KHA/Fe₃O₄ sample powders with the aid of Scherrer and Williamson-Hall equations [50] were calculated.

KHA Sol-gel Synthesis

First of all, triethyl phosphate ((C₂H₅O)₃PO, TEP) was hydrolyzed for 24 h at room temperature (R.T.) along with the vigorous stirring. Then, the aqueous solution of 3M Ca(NO₃)₂·4H₂O and 3M KNO₃ (28 w/w% K) were added to 4 M hydrolyzed TEP ((Ca + K)/P = 1.67) slowly at a rate of 6 ml min⁻¹. Next, the respected sol solution was vigorously mixed for 60 min at 80 °C. Finally, the obtained clear solution was aged for 48 h at R.T. In order to better following of gradually progress of sol-gel process, the pH values of sample solutions before and during aging were recorded. After that, the aged sol was dried at 100 °C until a white dried gel was obtained. The dried gel was ground into fine powder and then calcined at 700 °C for 1 h at a constant heat rate of 2 °C min⁻¹.

Fe₃O₄ and KHA/Fe₃O₄ Nanocomposite Synthesis

FeCl₂·4H₂O (0.13 g) and FeCl₃·6H₂O (0.37 g) were dissolved in deionized water (30 ml) and then 10 ml NH₃·H₂O was added along with mechanical stirring for 30 min at 50 °C. The prepared sample of Fe₃O₄ was collected by a magnet. A typical experiment procedure [51] for the hydrothermal synthesis of KHA/Fe₃O₄ with 50 wt% KHA content was used: 240 mg of KHA was dispersed into 40 ml of deionized water with 1 h of sonication. Then, 30 ml mixed solution (0.65 mmol of FeCl₂·4H₂O and 1.3 mmol of FeCl₃·6H₂O) was added drop-wise into it with 3 ml min⁻¹ rate along with 1 h stirring at R.T. In following, the mixture was adjusted to a pH of 11.0 with 6 M NaOH solution and stirred for 30 min. The resulting solution was transferred into a 200 ml Teflon-lined stainless steel autoclave, sealed and heated to 180 °C for 12 h. The reaction mixture was allowed to cool down to R.T., next the precipitate was filtered, washed with distilled water two times, and dried in an oven at 70 °C for 10 h.

Extraction Procedure

Firstly, 30 ml sample solution of PEs was placed into a glass vial, and the solution pH was adjusted to 7 with an

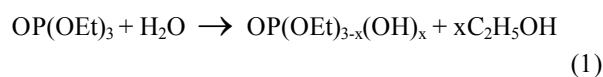
appropriate amount of 0.1 M HCl or NaOH. Then, 25 mg of KHA/Fe₃O₄ adsorbent was added to the solution and homogeneously dispersed with the aid of ultrasonication for 30 s and stirred vigorously for 8 min. After performing the extraction, a strong Nd-Fe-B magnet (2 × 2 × 1 cm, 1.4 T) was deposited at the bottom of the vial and supernatant water was decanted. The adsorbed analytes were eluted from the isolated sorbent with 200 μl dichloromethane by ultrasonication for 5 min. Finally, the magnetic adsorbent was collected *via* an external magnet and the desorbed analytes solution was analyzed using GC-FID for PEs determination.

RESULTS AND DISCUSSION

Characterization of KHA and KHA/Fe₃O₄

According to Fig. 1, the XRD pattern of synthesized KHA and KHA/Fe₃O₄ samples show the intense peaks of apatite (AP) structure, Fe₃O₄, and impurity phase of CaO which match the (JCPDS; No.: 01-084-1998). The indices of AP ((002) at 26, (211) at 32, (112) at 33, (300) at 34, (222) at 47, and (213) at 50°), Fe₃O₄ ((220) at 30, (311) at 35.5, (511) at 57, and (440) at 63°), and CaO ((200), at 37.4°) confirm the hexagonal, cubic, and cubic systems for them, respectively. Overall, synthesized KHA and KHA/Fe₃O₄ had a good and stable crystal shape.

Phosphorus alkoxide such as TEP are the known precursors for the preparation of sol-gel HA [52]. However, the more purified product could be obtained by better controlling the steps of the sol-gel process [47]. Herein, as advantages over other methods [53,54] doing the hydrolysis process of TEP (Eq. (1)) and in following the addition of Ca precursor, could be resulted in the more completed polymerization reaction of Ca and P (Eq. (2)). A continuous pH measurement of mixed solution of two precursor sols indicated that decreasing of pH value occurred from ~ 6.7 to 5.3 during aging of 24 h that confirmed by Eq. (2). In addition, the control of the heat treatment and aging steps of sol-gel route helps to improve the polymerization process between Ca, K and P precursors that resulted in reducing of the mentioned second phases [47].



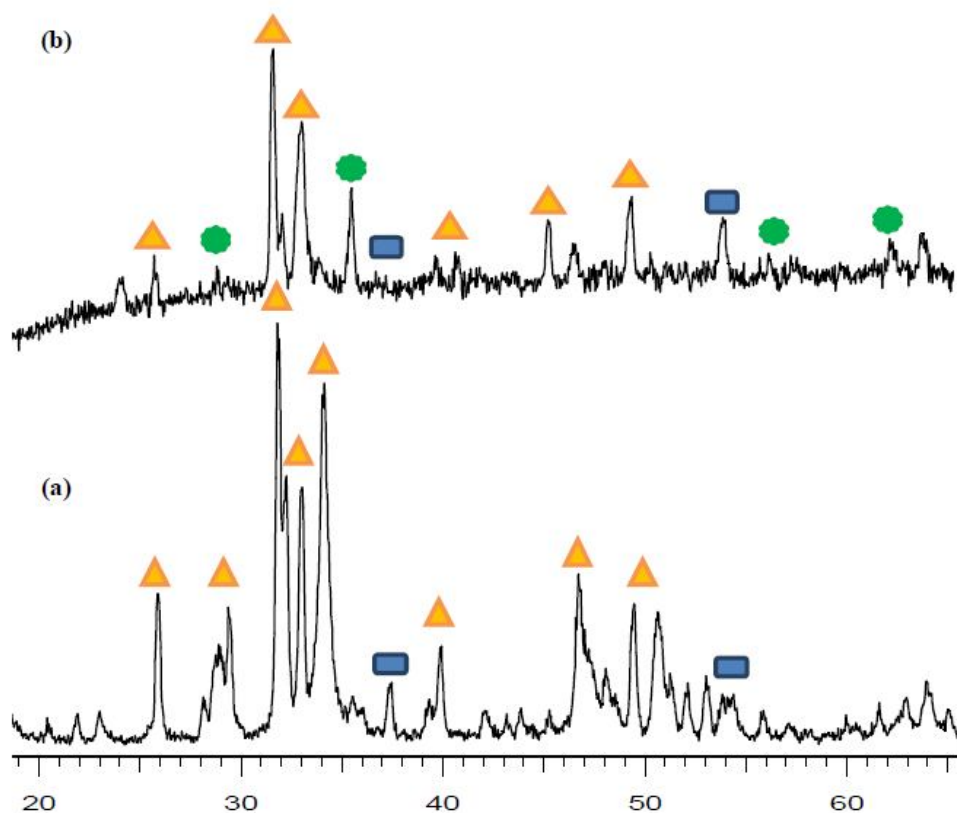
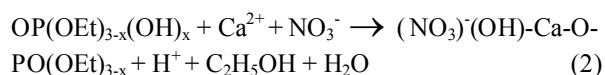


Fig. 1. (a) X-ray diffraction patterns of KHA calcined at 700 °C and (b) KHA/Fe₃O₄, shown: (▲) HA; (■) CaO; and (●) Fe₃O₄.



However, imperfect polymerization between Ca and P precursors (Eq. (2)) caused to calcium oxide (CaO) and calcium carbonate (CaCO₃) impurity formation (see Fig. 1).

FTIR spectra can explore the functional groups of particles surface of KHA (Fig. 2). In order to the comparison, the FTIR spectrum of KHA/Fe₃O₄ nanocomposite is also presented. The FTIR of calcined KHA sample at 700 °C shows the bands at 609, 890, 966-1170, assigned to stretching modes of phosphate, 1380-1460 and 1656 cm⁻¹ attributed to carbonate, and 3010-3600 related to adsorbed water and O-H functional group. The presence of carbonate in the structure of apatite claims a reason for high adsorption capacity of this synthesized KHA. The observed peaks are in good agreement with the

other reported data in the literature [55]. For KHA/Fe₃O₄ an index adsorption peak at 570 cm⁻¹ which is assigned to Fe-O bond confirm the presence of Fe₃O₄. Moreover, the bands at 3520 and 3643 cm⁻¹ is characteristic of O-H bond of the adsorbed water (see Fig. 2).

However, the sol-gel technique because of low temperatures of thermal treatments (including calcination) resulted in small particles of gells with high surface energy that concluded in the highly agglomerated crystal of them with significant porosity. Elemental analyses for the presence of Ca, K, P and Fe were made using Energy Dispersive X-ray Analysis (EDXA) (Philips PW2400 X-Ray Fluorescence Spectrometer). W/W%: KHA; K 28.7%, Ca 7.98%, P 11.7%, C 6.70%. KHA/Fe₃O₄; K 14.4%, Ca 4.0%, P 5.8%, C 3.4%, Fe 36.0%. The elemental analysis of EDXA confirmed the preparation of carbonate KHA with proposed (Ca_{2.04}K_{2.96})(PO₄)_{0.94}(CO₃)_{2.06}(OH)_{0.1}

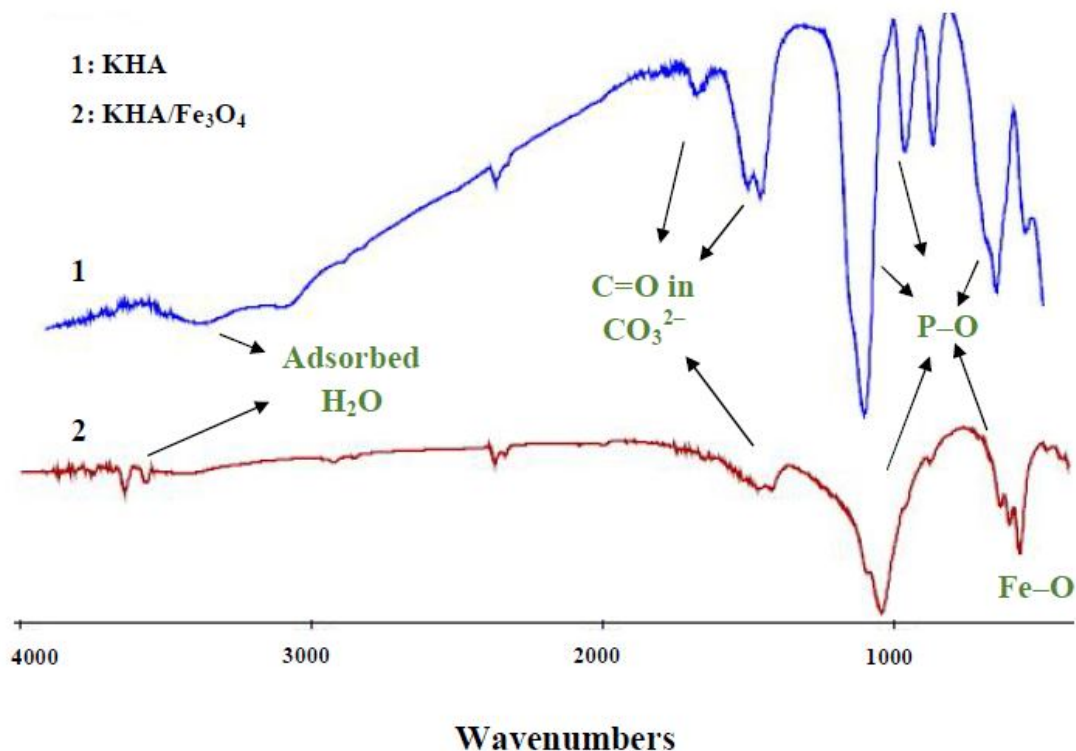


Fig. 2. FTIR of KHA calcined at 700 °C and KHA/Fe₃O₄ nanocomposite.

formula and 1.685 molar ratio of the (Ca + K)/P (see Fig. 3).

The same formula for KHA/Fe₃O₄ nanocomposite including the 50 wt% Fe₃O₄ should be suggested. The particle size of KHA and KHA/Fe₃O₄ using TEM as the direct method observed as 55-65 and 60-75 nm, respectively (see Figs. 4a and 4b). Also, XRD as an indirect method measured the related mean particle size of KHA and KHA/Fe₃O₄ as 57.3 and 64.7, respectively (see Figs. 4d and 4e). The Scherrer formula (Eq. (3)) using XRD pattern was applied for particle size measurement [47,56].

$$D = K\lambda/[W\text{Cos}\theta] \quad (3)$$

where K is a constant value of 0.9, λ is the Cu K α radiation (0.1544 nm), W is the full width at half-maximum, and θ is the diffraction angle (deg). However, the peak width of the XRD pattern changed in contributions with the crystallite size, micro-strain ϵ_s , and the instrument effect [56].

Therefore, for the deconvolution of instrumental and size of a particle, the more accurate Williamson-Hall (W-H)

method using the Cauchy approximation (Eq. (4)) was applied (For more information see the literature [47,50]).

$$(W\text{Cos}\theta) = (K\lambda/D) + 4\epsilon_s \text{Sin}\theta \quad (4)$$

Through drawing the curves of W-H of (WCos θ) vs. Sin θ for the mentioned miller indices of Fe₃O₄ and KHA in pure and nanocomposite compounds, the crystallite size (D) and ϵ_s of the related particles were specified. The measured results of W-H plots for KHA in pure and nanocomposite and Fe₃O₄ are D = 57.3, 64.7, and 18.4 nm and ϵ_s = 1.60 E-3, 1.75 E-4, and 1.83 E-3 (cf. Figs. 4d-f). According to TEM images (Figs. 4a-c), KHA particles in pure and nanocomposite samples are almost spherical in shape with an average diameter of near 60, and 65 nm, while particles of Fe₃O₄ have uniform shape with an average size of 18 nm that well distributed in between of apatite particles. This magnetic decoration avoids the agglomeration of KHA particles, resulted in increasing the active surface area of the new synthesized KHA/Fe₃O₄ compound.

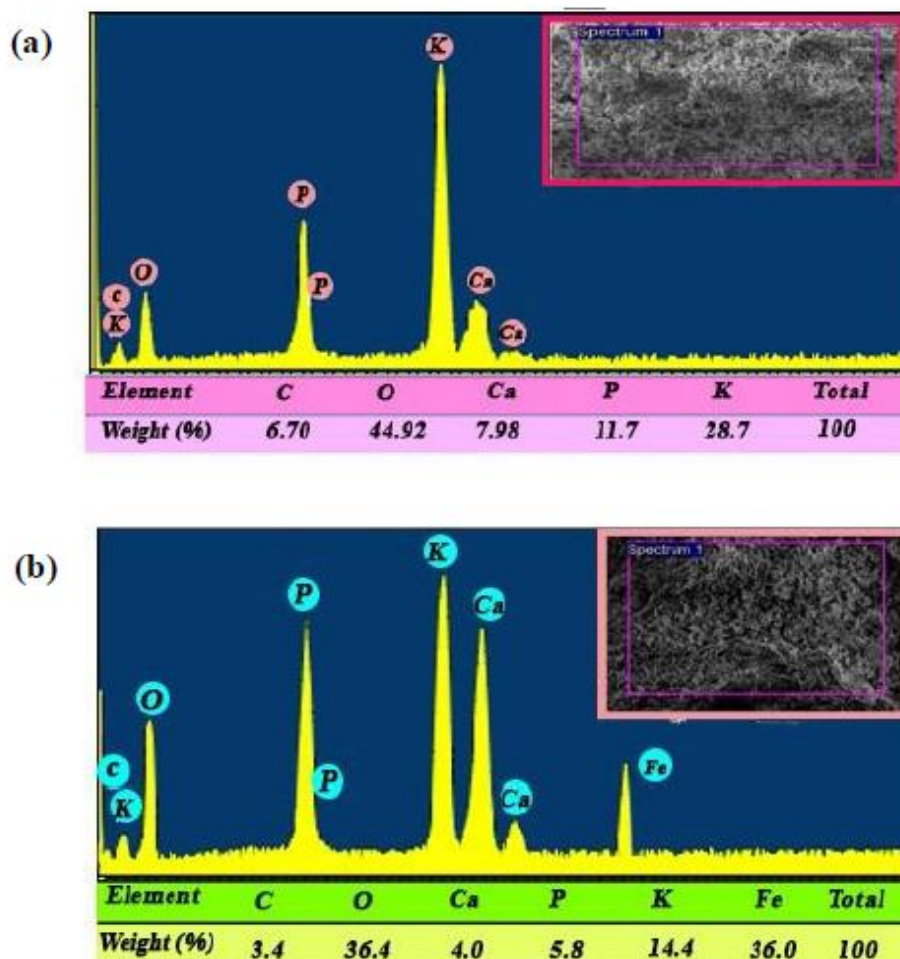


Fig. 3. EDXA results for KHA (a) and KHA/Fe₃O₄ (b).

Optimization of the MSPE Procedure

In order to obtain maximum achievable extraction efficiency, affecting parameters on the MSPE such as the amount of sorbent, desorption conditions, extraction time, and sample pH were screened and optimized.

The sorbent amount mass is a crucial factor that needs to be considered during the extraction process. To choose a suitable sorbent amount for enrichment of PEs, different amounts of KHA/Fe₃O₄ nanocomposite were tested in the range 5-30 mg. As can be seen in Fig. 5, the extraction efficiency improved as the amounts of KHA/Fe₃O₄ nanocomposite increased due to enhancement in the surface area and active sites. The maximum extraction efficiencies of all PEs were achieved using only

20 mg of the KHA/Fe₃O₄ nanocomposite, and adding more than 20 mg of the sorbent, the extraction efficiency did not significantly changed and almost remained constant. Therefore, the optimal sorbent amount was selected as 20 mg for further study.

To obtain satisfactory extraction efficiency, the selection of a proper solvent for desorption of analytes is quite necessary. In the present study, several eluents, such as acetonitrile, methanol, chloroform, acetone, and dichloromethane, were tested to select the best eluent solvent for eluting of PEs from the sorbent, and their extraction efficiencies were evaluated. The extraction efficiencies of these eluents are depicted in Fig. 6. The results clearly indicated that dichloromethane had the

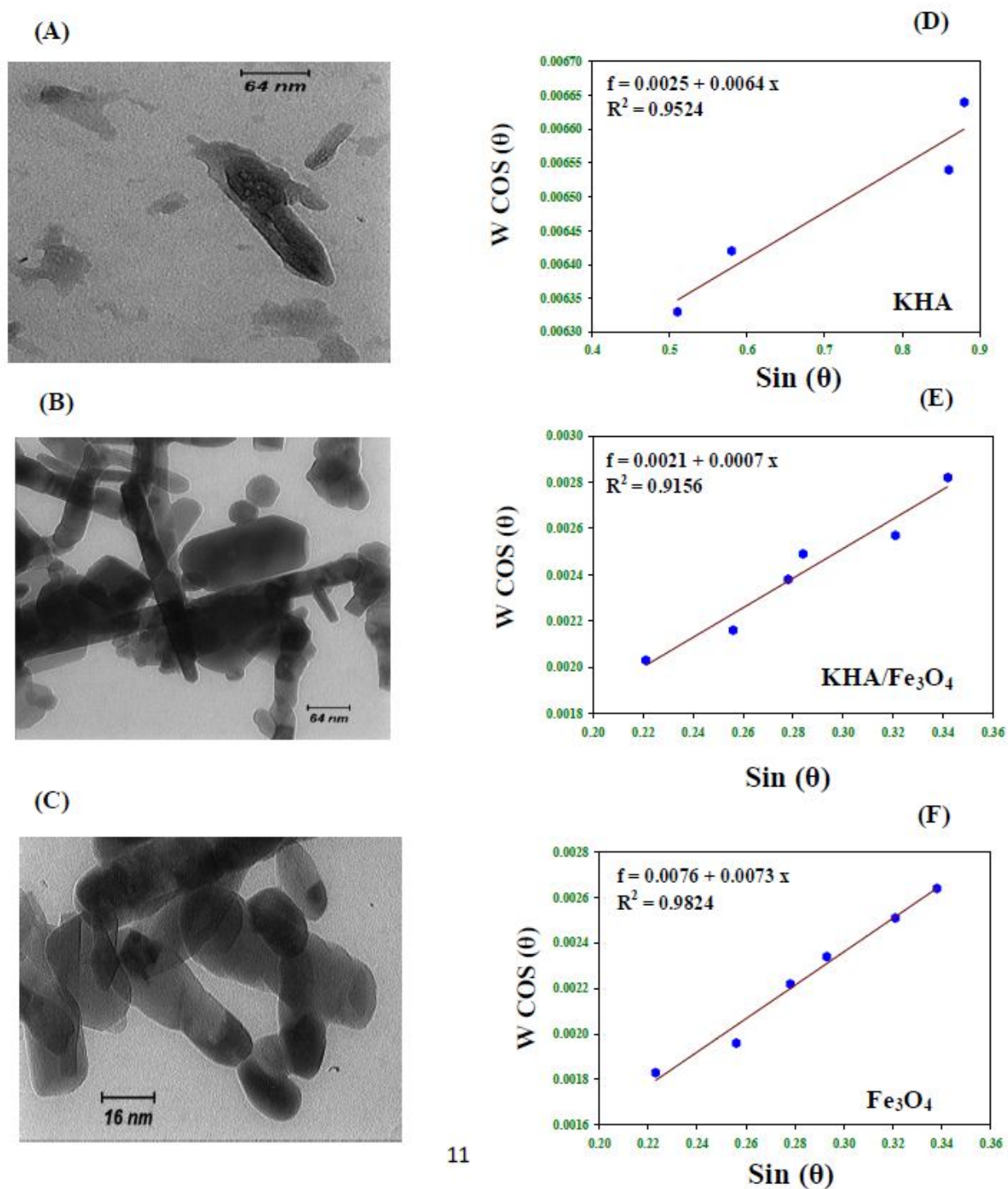


Fig. 4. TEM images of (a) KHA calcined at 700 °C, (b) KHA/Fe₃O₄ nanocomposite, (c) Fe₃O₄; and W-H plot drawn using Cauchy approximation for (d) KHA calcined at 700 °C, (e) KHA/Fe₃O₄ nanocomposite, and (f) Fe₃O₄.

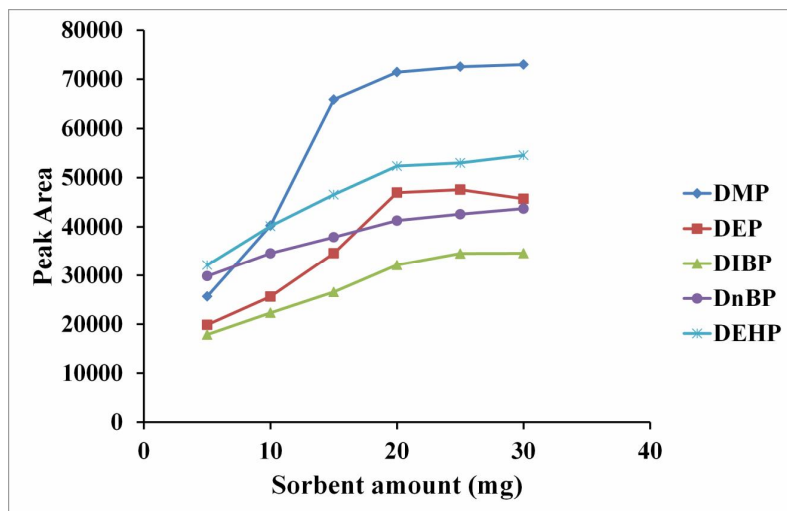


Fig. 5. Effect of sorbent amount on the extraction efficiency. Extraction conditions: sample volume, 30 ml; extraction time, 5 min; desorption solvent, methanol; volume of desorption solvent, 150 μ l; desorption time, 3 min; pH, 7.

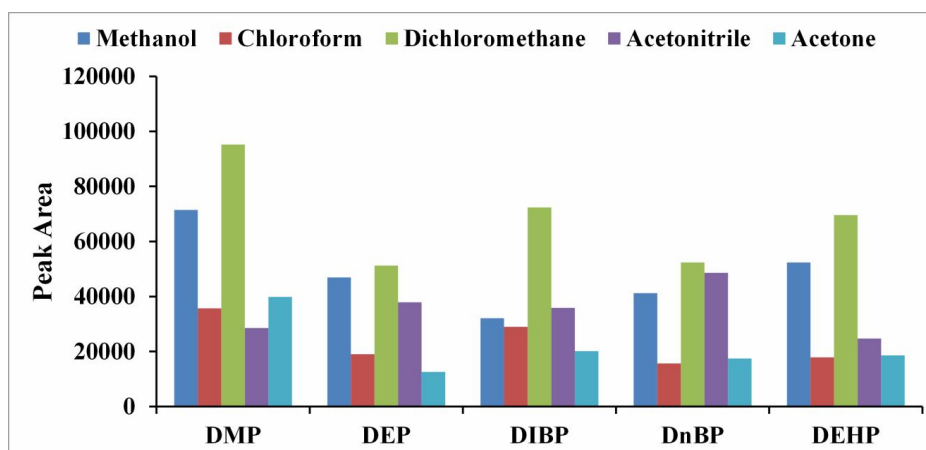


Fig. 6. Effect of desorption solvent on the extraction efficiency. Extraction conditions: sample volume, 30 ml; desorption time, 3 min; extraction time, 5 min; volume of eluent, 150 μ l; pH, 7.

highest recovery efficiency in comparison with other solvents. Therefore, dichloromethane was chosen as the elution solvent.

The pH value of sample solution plays an important role in the adsorption of target compounds by affecting the existing form of analytes, the charge species, and density on sorbents surface. Thus, the environmental water

samples were adjusted by 0.1 M HCl and NaOH solutions to form different pH values of 5, 6, 7, 8 and 9. The experimental results (Fig. 7) showed that the magnetic adsorbents gave the best performance in neutral solution. As a result, the sample solution was kept at its original pH value (pH = 7) for the following extractions.

Obtaining the minimum volume of eluent solvent is

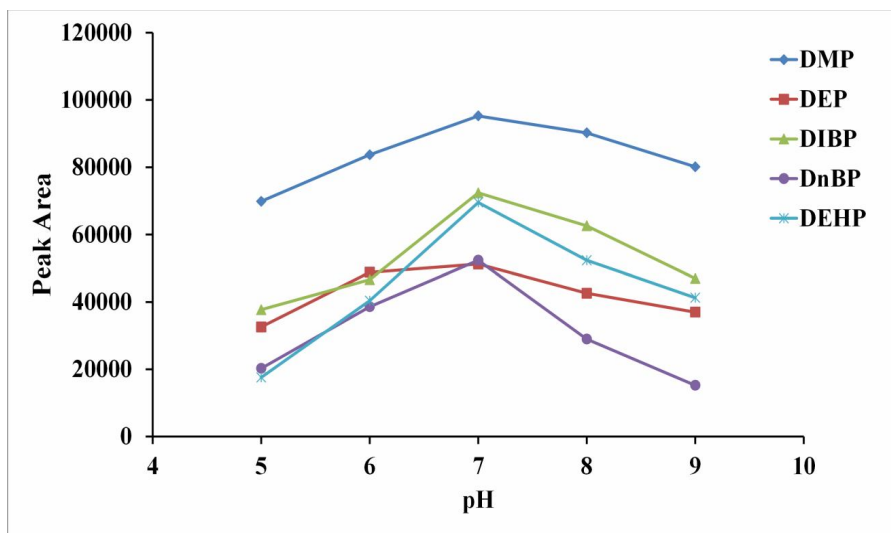


Fig. 7. Effect of pH on the extraction efficiency. Extraction conditions: sample volume, 30 ml; extraction time, 5 min; desorption solvent, 150 μ l dichloromethane; desorption time, 3 min.

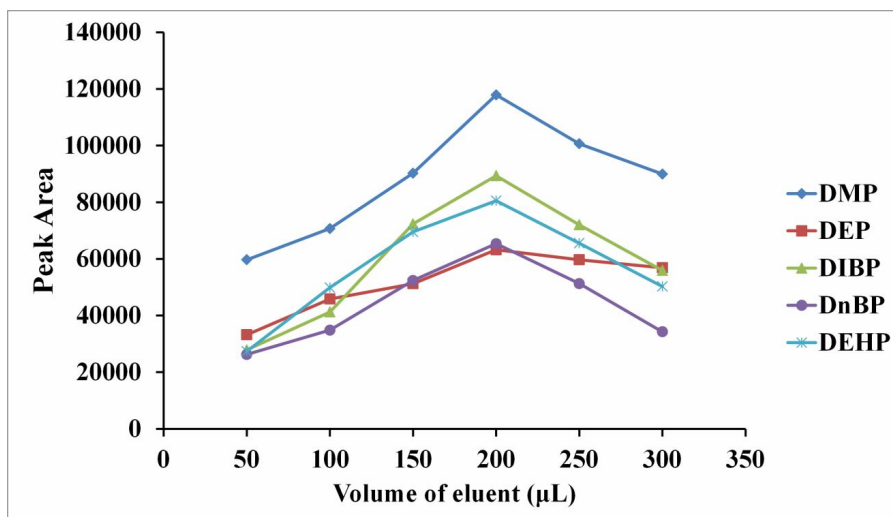


Fig. 8. Effect of volume of desorption solvent on the extraction efficiency. Extraction conditions: sample volume, 30 ml; desorption solvent, dichloromethane; desorption time, 3 min; extraction time, 5 min; pH, 7.

important to achieve the maximum preconcentration factor. Under the same experimental conditions, the effect of eluent volume on extraction efficiencies of target analytes was investigated in the volume range of 50-300 μ l (Fig. 8). The experimental results indicated that, 200 μ l of

dichloromethane as eluent is sufficient to obtain satisfactory recoveries and acceptable preconcentration factors for PEs.

To achieve satisfactory extraction efficiency, the influence of desorption time was investigated at time duration of 2, 3, 4, 5 and 6 min (Fig. 9). All peak areas of

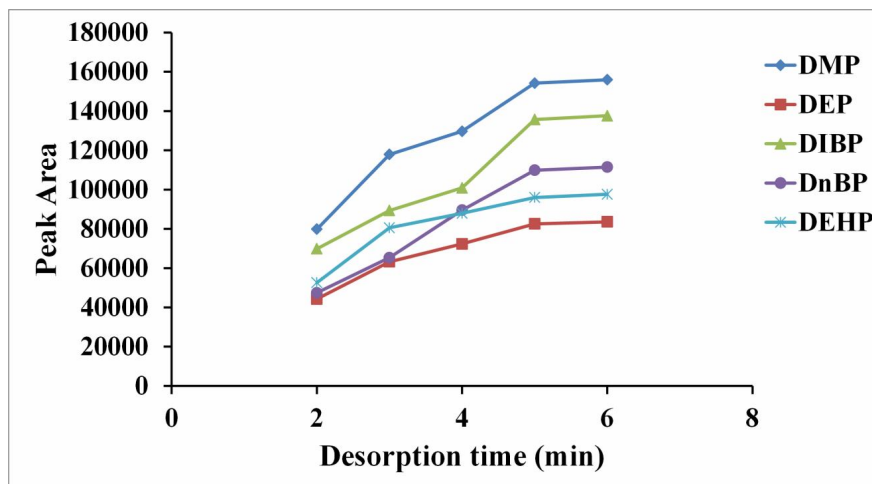


Fig. 9. Effect of desorption time on the extraction efficiency. Extraction conditions: sample volume, 30 ml; desorption solvent, 200 μ l dichloromethane; extraction time, 5 min; pH, 7.

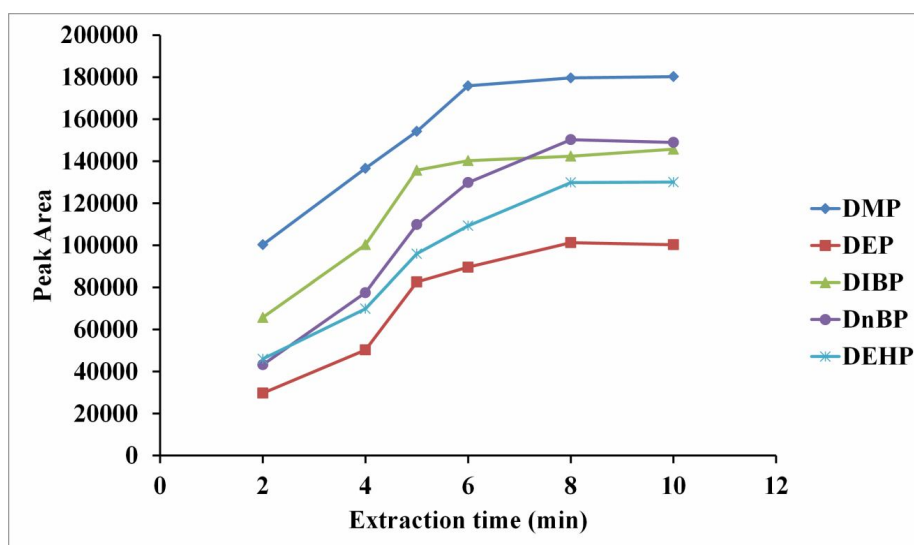


Fig. 10. Effect of extraction time on the extraction efficiency. Extraction conditions: sample volume, 30 ml; desorption solvent, 200 μ l dichloromethane; desorption time, 5 min; pH, 7.

target analytes evidently increased with increasing desorption time from 1 to 5 min. After 5 min, the peak area slightly varied or remained unchanged. Therefore, 5 min of desorption time was chosen based on the experimental results.

Extraction time is a key factor for pretreatment methods.

Thus, the time of extraction was optimized in the range of 2-10 min. According to the results display in Fig. 10, the peak area of the target analytes raised with extraction time increasing till 8 min. After 4 min, it reached a plateau, which suggested that 8 min was sufficient to reach equilibrium.

Table 1. Analytical Figures of Merit of the Method for the Extraction and Determination of the PEs

Analyte	Linear range (ng ml ⁻¹)	LOD (ng ml ⁻¹)	Correlation coefficient (r)	Within-day RSD% (n = 5) at three concentration (ng ml ⁻¹)			Between-day RSD% (n = 3)	EF	ER%
				0.1	5	50			
				DMP	0.015-70	0.005			
DEP	0.1-100	0.03	0.9969	5.8	5.1	4.2	6.9	76	50.6
DIBP	0.07-80	0.02	0.9950	6.5	5.8	5.5	6.8	82	54.7
DnBP	0.07-100	0.01	0.9942	8.1	6.9	6.3	8.9	85	56.6
DEHP	0.06-100	0.02	0.9945	5.7	5.0	4.9	6.3	90	60.0

Method Validation

Method calibration was performed by plotting the mean peak area obtained from three measurements versus sample concentration. The analytical data obtained are tabulated in Table 1. The calibration plots were linear over a concentration range of 0.015-70 ng ml⁻¹ for DMP, 0.1-100 ng ml⁻¹ for DEP, 0.07-80 ng ml⁻¹ for DIBP, 0.07-100 ng ml⁻¹ for DnBP, and 0.06-100 ng ml⁻¹ for DEHP. The regression coefficients varied between 0.9942-0.9986 and the detection limits, calculated as three times the signal-to-noise ratio were 0.005 ng ml⁻¹ for DMP, 0.03 ng ml⁻¹ for DEP, 0.02 ng ml⁻¹ for DIBP, 0.01 ng ml⁻¹ for DnBP and 0.02 ng ml⁻¹ for DEHP. The intra-day precision of the method, expressed as relative standard deviation (RSD%) was obtained using extracting five consecutive aqueous samples (spiked at three concentration levels of 0.1, 5 and 50 ng ml⁻¹ of analytes) and it was found to vary between 4.9 and 8.1%. The inter-day precision was determined by performing three consecutive extractions each day over a period of three working days. The water samples were spiked at 0.1 ng ml⁻¹. The inter-day RSDs varied from 6.3 to 8.9%. The enrichment factor (EF) and overall extraction recovery (ER%) were exploited to evaluate the efficiency of the MSPE method with KHA/Fe₃O₄ nanocomposite. The EF was defined as the ratio of the concentration of analyte in the final extracted phase (C_f) to the initial concentration of analyte (C₀) in the sample:

$$EF = \frac{C_f}{C_0}$$

The EFs of the method were 76-110. The ER% was defined as the percentage of total analyte moles (n₀) extracted to the extracted phase (n_f):

$$ER\% = \frac{n_f}{n_0} \times 100 = \frac{C_f}{C_0} \times \frac{V_f}{V_{aq}} \times 100$$

where V_f and V_{aq} are the eluent volume and aqueous sample volume, respectively. The absolute extraction recoveries were in the interval of 50.6-73.3%.

Analysis of Real Samples

The method was also applied in the analysis of two drinking water samples collected from the Sabzevar and Mashhad (Razavi Khorasan Province, Iran), river water, and bottled mineral water. Table 2 lists the quantitative results for the five target analytes in the environmental water samples. As can be seen, the low concentrations of PEs were detected in the real water samples. To validate the accuracy of the method, the water samples were spiked with three different concentration levels and recovery test was carried out. Table 2 also lists the relative recoveries for the spiked environmental water samples. It can be seen that the relative recoveries of 86.3-99.2% were obtained for five target phthalate esters in spiked water samples. So, it was

Table 2. Results of the Determination and Recoveries of PEs in Real Samples

Sample	Analyte	Mean (ng ml ⁻¹)	Spiked amount (ng ml ⁻¹)					
			0.1		5		50	
			Relative recovery (%)	RSD (%)	Relative recovery (%)	RSD (%)	Relative recovery (%)	RSD (%)
Tap water ^a	DMP	0.4	96.0	7.7	96.9	6.5	98.1	6.0
	DEP	0.2	97.9	6.3	98.2	5.9	98.6	5.8
	DIBP	ND	95.8	7.0	96.9	6.2	97.3	5.9
	DnBP	ND	96.5	8.2	97.2	7.8	97.6	7.5
	DEHP	0.8	95.5	6.2	96.0	5.9	96.3	5.9
Tap water ^b	DMP	0.2	97.5	7.1	98.1	6.6	98.4	6.5
	DEP	0.1	98.2	8.3	98.4	7.8	98.6	7.0
	DIBP	ND	96.9	7.2	97.4	6.7	98.0	6.5
	DnBP	ND	97.3	7.8	97.7	7.2	98.1	6.9
	DEHP	0.3	98.3	6.0	98.9	5.4	99.2	5.3
River water	DMP	5.9	91.6	8.6	93.4	8.0	94.9	7.8
	DEP	1.8	89.3	7.0	91.3	6.6	93.5	6.3
	DIBP	1.2	90.2	7.8	92.5	7.2	93.0	7.6
	DnBP	4.0	88.6	9.2	89.9	8.3	90.0	8.4
	DEHP	0.1	87.0	8.8	88.7	8.5	89.3	8.5
Bottled mineral water	DMP	3.5	92.2	7.3	95.6	6.6	96.2	6.7
	DEP	0.3	88.1	9.3	89.9	8.4	90.5	8.0
	DIBP	ND	86.3	7.6	87.6	7.1	88.0	6.8
	DnBP	ND	91.3	7.7	92.5	7.0	94.0	6.3
	DEHP	2.6	90.3	8.9	92.2	8.3	92.3	8.1

ND: Not detected. ^aDrinking water from Sabzevar, Iran. ^bDrinking water from Mashhad, Iran.

concluded that the matrices of the natural water samples had no significant influence on the extraction efficiency of this method.

Comparison of the Method with other Methods

The method was compared with a variety of techniques

recently represented in the literature for preconcentration and determination of PEs in water samples such as solid-based disperser liquid-liquid microextraction (SB-DLLME) [57], dynamic liquid-phase microextraction (Dynamic-LPME) [58], salting-out homogeneous liquid-liquid extraction (SHLLE) [59], DLLME [60], Solid-phase

Table 3. Comparison of the Developed method with other Methods for Determination of PEs in Water Samples

Method	Detection system	LOD (ng ml ⁻¹)	Linear range (ng ml ⁻¹)	RSD (%)	Ref.
SB-DLLME	GC-FID	0.09-0.25	0.5-2000	2.5-4.5	[57]
Dynamic-LPME	GC-FID	0.43-4.30	5-5000	5.3-6.4	[58]
SHLLE	GC-FID	0.02-0.7	1-5000	3-8	[59]
DLLME	GC-FID	1.0-1.1	-	4-5	[60]
SPME	GC-FID	0.05-0.12	0.4-600	4.1-6.8	[61]
SPME	GC-FID	0.042-0.26	0.1-245	8.2-16	[62]
MSPE	GC-FID	0.2-0.4	0.4-100	4.0-12.3	[63]
MEPS	GC-FID	0.02-0.1	0.25-100	4.8-8.3	[25]
MSPE	GC-FID	0.005-0.03	0.015-100	4.9-8.1	This study

microextraction (SPME) [61,62], MSPE [63], and microextraction in packed syringe (MEPS) [25]. The distinct characteristics of the suggested method are summarized in Table 3. Large linear dynamic ranges and very low LODs are important features of the method in comparison with those techniques. In addition, the RSD% of the method is comparable to (or even better than) the RSDs% of some of the above techniques. All these results reveal that the MSPE method based on KHA/Fe₃O₄ nanocomposite is an ultra-sensitive, rapid, and reproducible method, which can be exploited as a routine method for ultra-preconcentration of PEs in aqueous samples.

CONCLUSIONS

In the present work, using an easy low temperature sol-gel technique, the nano-particles of potassium substituted HA (KHA) and in following the magnetic KHA/Fe₃O₄ nanocomposite were synthesized and then the structural evolution and particle size evaluation using XRD, FTIR, EDXA, and TEM analyses were investigated. The modified Scherrer's equation and TEM images show the determined 60, 65 and 18 nm as the average particle size of KHA,

KHA/Fe₃O₄, and Fe₃O₄, respectively. The synthesized KHA/Fe₃O₄ nanocomposite can be employed as low-cost and effective sorbent for extraction of phthalate esters from water samples. Under the optimal conditions (sample pH, 7; amount of sorbent, 25 mg; extraction time, 8.0 min; desorption solvent and its volume, 200 μ l dichloromethane; and desorption time, 5.0 min) good linearity, low limits of detection, and satisfactory spiked recoveries were attained for the real samples. Taken together, the KHA/Fe₃O₄ nanocomposite may serve as a promising alternative to the present sorbent available.

ACKNOWLEDGMENTS

MC and AA gratefully acknowledge the financial support by the Hakim Sabzevari University, Sabzevar, IRAN.

REFERENCES

- [1] C.A. Staples, D.R. Peterson, T.F. Parkerton, W.J. Adams, *Chemosphere* 35 (1997) 667.
- [2] D. Balafas, K.J. Shaw, F.B. Whitfield, *Food Chem.* 65

- (1999) 279.
- [3] S. Jobling, T. Reynolds, R. White, M.G. Parker, J.P. Sumpter, *Environ. Health Persp.* 103 (1995) 582.
- [4] C.A. Stales, D.R. Peterson, T.F. Parkerton, W.J. Adams, *Chemosphere* 35 (1997) 667.
- [5] P.M. Foster, R.C. Cattley, E. Mylchreest, *Food Chem. Toxicol.* 38 (2000) 97.
- [6] L.E. Gray, J. Ostby, J. Furr, M. Price, D.N.R. Veeramachaneni, L. Parks, *Toxicol. Sci.* 58 (2000) 350.
- [7] W.J. Adams, G.R. Biddinger, K.A. Robillard, J.W. Gorsuch, *Environ. Toxicol. Chem.* 14 (1995) 1569.
- [8] B.V. Chang, C.M. Yang, C.H. Cheng, S.Y. Yuan, *Chemosphere* 55 (2004) 533.
- [9] I. Ostrovský, R. Čabala, R. Kubinec, R. Górová, J. Blaško, J. Kubincová, L. Řimnáčová, W. Lorenz, *Food Chem.* 124 (2011) 392.
- [10] Q. Wu, M. Liu, X. Ma, W. Wang, C. Wang, X. Zang, Z. Wang, *Microchim. Acta* 177 (2012) 23.
- [11] Q. Xu, X. Yin, S. Wu, M. Wang, Z. Wen, Z. Gu, *Microchim. Acta* 168 (2010) 267.
- [12] S. Lirio, C.-W. Fu, J.-Y. Lin, M.-J. Hsu, H.-Y. Huang, *Anal. Chim. Acta* 927 (2016) 55.
- [13] E. Psillakis, N. Kalogerakis, *J. Chromatogr. A* 999 (2003) 145.
- [14] J.I. Cacho, N. Campillo, P. Vinas, M. Hernandez-Cordoba, *J. Chromatogr. A* 1241 (2012) 21.
- [15] Y. Yamini, M. Faraji, M. Adeli, *Microchim. Acta* 182 (2015) 1491.
- [16] A. Amiri, F.M. Zonoz, A. Targhoo, H.R. Saadati-Moshtaghin, *Microchim. Acta* 184 (2017) 1093.
- [17] A. Amiri, M. Baghayeri, M. Kashmari, *Microchim. Acta* 183 (2016) 149.
- [18] A. Matsushima, N. Kotobuki, M. Tadokoro, K. Kawate, H. Yajima, Y. Takakura, H. Ohgushi, *Artif. Organs* 33 (2009) 474.
- [19] G.D. Venkatasubbu, S. Ramasamy, V. Ramakrishnan, J. Kumar, *Biotechnology* 1 (2011) 173.
- [20] P. Tschoppe, D.L. Zandim, P. Martus, A.M. Kielbassa, *J. Dent.* 39 (2011) 430.
- [21] G. Li, L. Ye, J. Pan, M. Long, Z. Zhao, H. Yang, J. Tian, Y. Wen, S. Dong, J. Guan, B. Luo, *Liver Int.* 32 (2012) 998.
- [22] Y. Cai, Y. Liu, W. Yan, Q. Hu, J. Tao, M. Zhang, Z. Shi, R. Tang, *J. Mater. Chem.* 17 (2007) 3780.
- [23] Y. Boonsongrit, H. Abe, K. Sato, M. Naito, M. Yoshimura, H. Ichikawa, Y. Fukumori, *Mat. Sci. Eng. B* 148 (2008) 162.
- [24] F. Zhang, B. Ma, X. Jiang, Y. Ji, *Powder Technol.* 302 (2016) 207.
- [25] A. Amiri, M. Chahkandi, A. Targhoo, *Anal. Chim. Acta* 950 (2017) 64.
- [26] G. Bharath, N. Ponpandian, *RSC Adv.* 5 (2015) 84685.
- [27] M.I. Kay, R.A. Young, *Nature (London)* 204 (1964) 1050.
- [28] K.G. Scheckel, G.L. Diamond, M.F. Burgess, J.M. Klotzbach, M. Maddaloni, B.W. Miller, C.R. Partridge, S.M. Serda, *J. Toxicol. Environ. Health B Crit. Rev.* 16 (2013) 337.
- [29] K.L. Lin, J.Y. Pan, Y.W. Chen, R.M. Cheng, X.C. Xu, *J. Hazard. Mater.* 161 (2009) 231.
- [30] Y. Tang, H.F. Chappell, M.T. Dove, R.J. Reeder, Y.J. Lee, *Biomater.* 30 (2009) 2864.
- [31] G. Liu, J.W. Talley, C. Na, S.L. Larson, L.G. Wolfe, *Environ. Sci. Technol.* 44 (2010) 1366.
- [32] H.P. Wiesmann, U. Plate, K. Zierold, H.J. Höhling, *J. Dent. Res.* 77 (1998) 1654.
- [33] C. Srilakshmi, R. Saraf, *Micropor. Mesopor. Mat.* 219 (2016) 134.
- [34] W. Chen, Z. Huang, Y. Liu, Q. He, *Catal. Commun.* 9 (2008) 516.
- [35] E.S. Bogya, R. Barabas, A. Savdari, V. Dejeu, I. Baldea, *Chem. Pap.* 63 (2009) 568.
- [36] C.H. Suelter, *Science* 168 (1970) 789.
- [37] H.J. Hohling, H. Mishima, Y. Kozawa, T. Daimon, R.H. Barckhaus, K.D. Richter, *Scanning Microsc. Int.* 5 (1991) 247.
- [38] S. Kannan, J.M.G. Ventura, J.M.F. Ferreira, *Ceram. Int.* 33 (2007) 1489.
- [39] D.G. Shchukin, G.B. Sukhorukov, H. Möhwald, *Chem. Mater.* 15 (2003) 3947.
- [40] S.P. Nukavarapu, S.G. Kumbar, J.L. Brown, N.R. Krogman, A.L. Weikel, M.D. Hindenlang, L.S. Nair, H.R. Allcock, C.T. Laurencin, *Biomacromolecules* 9 (2008) 1818.
- [41] X. Gao, J. Song, P. Ji, X. Zhang, X. Li, X. Xu, M. Wang, S. Zhang, Y. Deng, F. Dengand, S. Wei, *ACS*

- Appl. Mater. Interfaces 8 (2016) 3499.
- [42] L. Jiang, Y. Li, C. Xiong, S. Su, H. Ding, ACS Appl. Mater. Interfaces 9 (2017) 4890.
- [43] J. Zhang, H. Liu, J.-X. Ding, J. Wu, X.-L. Zhuang, X.-S. Chen, J.-C. Wang, J.-B. Yinand, Z.-M. Li, ACS Biomater. Sci. Eng. 2 (2016) 1471.
- [44] W. Gan, L. Gao, X. Zhan, J. Li, RSC Adv. 5 (2015) 45919.
- [45] K. Pandi, N. Viswanathan, J. Chem. Eng. Data 61 (2016) 571.
- [46] M. Liu, H. Liu, S. Sun, X. Li, Y. Zhou, Z. Houand, J. Lin, Langmuir 30 (2014) 1176.
- [47] H. Eshtiagh-Hosseini, M.R. Housaindokht, M. Chahkandi, Mater. Chem. Phys. 106 (2007) 310.
- [48] H. Eshtiagh-Hosseini, M.R. Housaindokht, M. Chahkandi, A. Youssefi, J. Non-Crys. Sol. 354 (2008) 3854.
- [49] M. Chahkandi, M. Mirzaei, J. Iran Chem. Soc. 14 (2017) 567.
- [50] A. Weibel, R. Bouchet, F. Boule'h, P. Knauth, Chem. Mater. 17 (2005) 2378.
- [51] Y. Fu, Q. Chen, M. He, Y. Wan, X. Sun, H. Xia, X. Wang, Ind. Eng. Chem. Res. 51 (2012) 11700.
- [52] K.A. Gross, C.S. Chai, G.S.K. Kannangara, B. Bin-Nissan, L. Hanley, J. Mater. Sci. Mater. Med. 9 (1998) 839.
- [53] K. Cheng, W. Weng, G. Han, P. Du, G. Shen, J. Yang, J.M.F. Ferreira, Mater. Chem. Phys. 78 (2003) 767.
- [54] K. Cheng, W. Weng, G. Han, P. Du, G. Shen, J. Yang, J.M.F. Ferreira, Mater. Res. Bull. 38 (2003) 89.
- [55] L. Cui, Y. Wang, L. Hu, L. Gao, B. Du, Q. Wei, RSC Adv. 5 (2015) 9759.
- [56] H. Borchert, E.V. Shevchenko, A. Robert, I. Mekis, A. Kornowski, G. Grübel, H. Weller, Langmuir 21 (2005) 1931.
- [57] M.A. Farajzadeh, P. Khorram, A.A.A. Nabil, J. Sep. Sci. 37 (2014) 1177.
- [58] J. Xu, P. Liang, T. Zhang, Anal. Chim. Acta 597 (2007) 1.
- [59] M.A. Farajzadeh, S. Sheykhizadeh, P. Khorram, J. Sep. Sci. 36 (2013) 939.
- [60] Y. Hongyuan, B. Liu, D.U. Jingjing, Kyung H.-R. Kyung, Analyst 135 (2010) 2585.
- [61] M.H. Banitaba, S.S.H. Davarani, A. Pourahadi, J. Chromatogr. A 1283 (2013) 1.
- [62] M. Jafari, H. Ebrahimzadeh, M.H. Banitaba, S.S.H. Davarani, J. Sep. Sci. 37 (2014) 3142.
- [63] E. Tahmasebi, Y. Yamini, M. Moradi, A. Esrafil, Anal. Chim. Acta 770 (2013) 68.